Singh et al | Article 11162
J Pure Appl Microbiol. 2026;20(3):2619-2639. doi: 10.22207/JPAM.20.3.57
Received: 20 November 2025 | Accepted: 04 June 2026
Published Online: 03 September 2026

P-ISSN: 0973-7510; E-ISSN: 2581-690X

RESEARCH ARTICLE OPEN ACCESS

In Silico Identification of Cinnamonol as a Potential FAS-II Pathway Inhibitor Targeting Mycolic Acid Biosynthesis in *Mycobacterium tuberculosis* from Phytochemicals Present in *Hawan Samagri*

Jagriti Singh[1], Vinny Virdi[1], Kratika Singh[2], Rolee Sharma[1] and Dipesh Kumar Verma[1]*

[1]Department of Life Sciences and Biotechnology, Chhatrapati Shahu Ji Maharaj University, Kanpur, Uttar Pradesh, India.
[2]Department of Data Sciences, Centre of Biomedical Research SGPGI, Lucknow, Uttar Pradesh, India.

Abstract

Tuberculosis (TB), caused by *Mycobacterium tuberculosis* (*M.tb*) infection, is increasingly challenged by the emergence of multidrug-resistant strains, necessitating the development of novel therapeutic strategies. This study aimed to identify natural phytochemicals from *Hawan Samagri*, a traditional Ayurvedic polyherbal mixture, with the potential to inhibit multiple enzymes of the fatty acid synthase II (FAS-II) pathway, a critical target for mycolic acid biosynthesis in *M.tb*. Plants constituting *Hawan Samagri* were first identified through Ayurvedic literature and subsequently screened using Dr. Duke's Phytochemical and Ethnobotanical Database to retrieve reported phytochemicals. Compounds not previously reported for antimycobacterial activity were selected and further filtered using Lipinski's Rule of Five and ADMET analysis. These shortlisted phytochemicals were then subjected to molecular docking against three key FAS-II enzymes-HadAB, FabG1, and KasA followed by molecular dynamics (MD) simulations to evaluate binding stability and interactions with catalytic and cofactor-binding residues. The analysis identified five promising compounds Cinnamonol, Episesamin, Norhyoscine, Apohyoscine, and Chrysophanol exhibiting strong binding affinities and stable interactions across the targeted enzymes. Among these, Cinnamonol demonstrated the most significant multitarget binding potential along with high stability during extended molecular dynamics simulations, indicating its promise as a broad-spectrum FAS-II inhibitor. Overall, this integrative in silico approach provides scientific validation for the traditional use of *Hawan Samagri* by identifying and characterizing its phytochemicals as potential multitarget inhibitors of the FAS-II pathway in *M.tb*, with Cinnamonol emerging as a particularly promising lead candidate for future anti-TB drug development due to its favorable pharmacokinetic properties and mechanistic relevance to fatty acid metabolism.

Keywords: *Mycobacterium tuberculosis*, FAS-II pathway, HadAB, KasA, FabG1, Herbal Compounds, Molecular Docking, Molecular Dynamics Simulation

***Correspondence:** dipeshverma@csjmu.ac.in

Citation: Singh J, Virdi V, Singh K, Sharma R, Verma DK. In Silico Identification of Cinnamonol as a Potential FAS-II Pathway Inhibitor Targeting Mycolic Acid Biosynthesis in *Mycobacterium tuberculosis* from Phytochemicals Present in *Hawan Samagri*. *J Pure Appl Microbiol.* 2026;20(3):2619-2639. doi: 10.22207/JPAM.20.3.57

INTRODUCTION

Tuberculosis (TB) caused by *Mycobacterium tuberculosis* (*M.tb*), a chronic granulomatous infectious disease that remains a global health problem. According to the WHO Global Tuberculosis Report 2024, an estimated 10.6 million new TB cases were reported in 2023, with more than 1.3 million deaths, emphasizing the ongoing burden of the disease.[1,2] The emergence of multidrug-resistant and extensively drug-resistant strains of *M.tb* has further complicated treatment and reduced the effectiveness of standard chemotherapeutic drugs such as isoniazid (INH) and rifampicin.[3] This growing resistance highlights the urgent need for novel therapeutic agents that target new biological pathways or enzymes not yet affected by resistance mechanisms.

One key factor contributing to *M.tb* pathogenicity and drug resistance is its highly complex lipid-rich cell wall, primarily due to the presence of mycolic acids, which are essential for cell wall integrity, immune evasion, and survival under stress conditions.[4] The biosynthesis of mycolic acids involves two fatty acid synthesis pathways: the eukaryotic-like FAS-I and the prokaryotic FAS-II systems.[5,6] The FAS-I system in mycobacteria synthesizes short- and medium-chain acyl-CoAs (C_{16}-C_{24}), which are subsequently elongated by the FAS-II system to generate very-long-chain meromycolic acids (C_{60}-C_{90}) required for mycolic acid biosynthesis. The FAS-II system is not unique to mycobacteria, it is widely distributed and is also found in many Gram-positive and Gram-negative bacteria (e.g. *E. coli* and *Bacillus subtilis*, etc.), plants, and in some apicomplexan parasites such as *Plasmodium falciparum*. However, in mycobacteria, the FAS-II pathway plays a specialized and critical role in the elongation of fatty acids required for mycolic acid biosynthesis, which is an essential component of the mycobacterial cell wall. In contrast, animals do not have the FAS-II pathway and only on the FAS-I system for *de novo* lipid synthesis. Plants, on the other hand, primarily utilize the FAS-II system within plastids and chloroplasts for fatty acid biosynthesis. This unique function of the FAS-II system in mycolic acid synthesis in mycobacteria makes it a promising target for drug discovery against *M.tb*.

The FAS-II system of mycobacteria includes four critical enzymes: β-hydroxyacyl-ACP dehydratase (HadAB), β-ketoacyl-ACP reductase (FabG1/MabA), β-ketoacyl-ACP synthase I, (KasA) and the NADH-dependent enoyl-ACP reductase (InhA).[7] Together, these enzymes sequentially catalyze condensation, reduction, dehydration, and final reduction reactions involved in fatty acid maturation required for cell wall biosynthesis.[8] Among all four enzymes, InhA has been the most widely studied, as it serves as the primary target of the frontline drug INH. However, mutations in the *katG* gene or regulatory regions of InhA have severely affected the efficacy of this pathway.[9] As a result, other FAS-II enzymes such as HadAB, FabG1, and KasA, which are for mycobacterial survival, structurally conserved, and lack human homologs, are now considered highly attractive yet underutilized drug targets.

In recent years several inhibitors have been discovered targeting FAS-II pathway.[10-13] Compounds including Thiolactomycin, Cerulenin, Platensimycin, and GSK3011724A have shown inhibitory activity against FAS-II enzymes. However, despite their promising in vitro activity, none of these compounds have progressed successfully to clinical use due to limitations in solubility, toxicity, or unfavorable pharmacokinetic properties.[10-13] These limitations highlight the urgent need to identify novel inhibitors with improved pharmacokinetic and safety profiles.[14,15]

In this context, several recent studies have demonstrated the potential of computational methods to targeting FAS-II pathway enzymes, identifying natural or synthetic inhibitors. Molecular docking and structure-based analysis to identify potential FAS-II inhibitors, demonstrating strong binding affinity and stable interactions with key catalytic residues. Such findings underscore the reliability of in silico approaches in screening and prioritizing candidate molecules targeting FAS-II enzymes. Collectively, these studies establish the FAS-II pathway as a promising target in anti-TB drug discovery.

Natural products, especially phytochemicals, have been reported as a rich source of therapeutic agents due to their structural diversity and biological significance. In this context, the traditional use of phytochemicals provides a unique and underexplored chemical space

for modern drug discovery.[16] *Hawan Samagri*, a ritualistic Ayurvedic mixture composed of aromatic resins, seeds, leaves, fruits, stems, and barks from *Himalayan* plant species, has long been used in spiritual fumigation and traditional medicine.[17,18] Preliminary studies suggest that the fumes of *Hawan Samagri* released after combustion contain potent antimicrobial properties, including inhibitory effects on *M.tb* Vapours of cinnamaldehyde, eugenol, and related phenylpropanoids have been reported to exhibit airborne antibacterial activity in vitro, suggesting that volatile constituents or their thermal derivatives may retain bioactivity even after combustion. However, the specific molecular components responsible for this bioactivity and its mechanisms of action remain largely unknown.[19]

Based on this rationale, forty-nine phytochemicals were selected from these twenty-seven *Himalayan herbs* and spices and computationally screened against three essential *M.tb* enzymes using structure-based virtual screening methods, along with drug-likeness filtration, ADMET profiling, molecular docking, and molecular dynamics simulations. Among the screened phytochemicals, Cinnamonol emerged as the most potent multitarget inhibitor, showing high binding affinity, stable interactions, and favorable pharmacokinetic properties.[10-13] Chrysophanol, Episesamin, Norhyoscine, and Apohyoscine demonstrated specificity toward individual enzymes, indicating target-selective activity.[20] Importantly, this integrative in silico approach provides scientific support for the traditional use of *Hawan Samagri* by identifying its constituent phytochemicals as potential multitarget inhibitors of the FAS-II pathway in *M.tb*. The strong binding affinity of Cinnamonol toward key FAS-II enzymes, along with its stable behavior observed during molecular dynamics simulations, suggests its potential to interfere with mycolic acid biosynthesis. These findings highlight Cinnamonol as a promising lead compound for further exploration in anti-TB drug development.[19,21]

MATERIALS AND METHODS

Ligand selection and preparation

The selection of ligands was initiated through the identification of plant species traditionally incorporated into *Hawan Samagri* formulations, with particular emphasis on herbs and spices predominantly grown in the *Himalayan* region. It is acknowledged that *Hawan Samagri* compositions may vary geographically and culturally; therefore, the present study represents a defined ethnobotanical subset rather than an exhaustive catalog of all possible constituents. A consolidated list of reported phytochemicals was generated for each plant. From this dataset, compounds were shortlisted based on the following criteria: (i) documented occurrence in the selected *Himalayan* medicinal plants, (ii) reported antimicrobial or pharmacological relevance in the literature, (iii) representation of diverse chemical classes, and (iv) likelihood of release, volatility, or persistence during fumigation processes. Only compounds not previously reported with established antimycobacterial activity were included to ensure novelty in the screening approach. This methodical process led to the creation of a curated library of forty-nine unique phytochemicals from twenty-seven plant species used in *Hawan Samagri*.[22] The three-dimensional structures of all phytochemicals were downloaded in SDF format from the PubChem database and converted into PDB format using BIOVIA Discovery Studio.[23] Ligands were subsequently converted to PDBQT format using AutoDock Tools (version 4.2.6),[24,25] with assigned Gasteiger charges and rotatable bonds.

Lipinski's Rule and ADMET prediction

All ligands were subjected to Lipinski's Rule of Five analysis to assess drug-likeness using the SCFBio-IITD online platform (http://www.scfbio-iitd.res.in).[26] Parameters such as molecular weight (<500 Da), logP (<5), hydrogen bond donors (≤5), and hydrogen bond acceptors (≤10) were evaluated. ADMET properties were predicted using PreADMET. Parameters assessed included human intestinal absorption (HIA), blood-brain barrier (BBB) permeability, cytochrome P450 inhibition, plasma protein binding (PPB), Ames mutagenicity, hepatotoxicity and carcinogenicity.[27] Compounds with high mutagenicity or carcinogenicity potential were excluded from further screening to ensure improved translational potential.

Table 1. Lipinski rule of five and ADMET properties of selected compound

No.	Compounds	Screened compounds following the drug-likeliness test					ADMET profiling of the filtered compounds							
		Molecular Mas	Xlog P3(<5)	H donor (≤5)	H acceptor (≤10)	Molar Refractivity (40-130)	Mutagenicity (Ames Test)	Carcinogenicity	HIA %	Pcaco-2 (nm/s)	Pmdck (nm/s)	Pski (nm/s)	PPB %	BBB %
1.	Cinnamonol	370	2.7	1	7	88.1	Mutagen	Non-carcinogenic	96.71	37.30	17.95	-4.43	78.45	0.02
2.	Episesamin	354	3.0	0	6	87.3	Mutagen	Non-carcinogenic	97.95	57.02	20.60	-4.42	83.12	0.05
3.	Norhyoscine	289	1.4	2	5	73.6	Mutagen	Non-carcinogenic	92.06	20.49	1.41	-4.66	18.72	0.02
4.	Apohyoscine	285	1.8	0	3	74.5	Mutagen	Non-carcinogenic	98.02	53.50	49.45	-3.96	35.00	0.02
5.	Chrysophanol	254	1.6	2	4	61.7	Mutagen	Non-carcinogenic	93.74	16.33	43.05	-3.46	100.00	0.71

Target Protein Retrieval and Preparation

Crystal structures of HadAB (PDB ID: 4RLJ; 1.75 Å resolution), FabG1 (PDB ID: 1UZN; 1.91 Å resolution), and KasA (PDB ID: 4C6U; 2.4 Å resolution) were retrieved from the RCSB Protein Data Bank.[28-30] Although the enzyme complex is referred to as HadAB, the catalytic dehydratase activity is primarily associated with the HadB subunit. Accordingly, molecular docking was performed on the HadB catalytic region within the HadAB complex structure. For each protein, only the biologically relevant monomeric chains were retained, and heteroatoms, water molecules, and bound ligands were removed to eliminate crystallographic artifacts using BIOVIA Discovery Studio.[31] The prepared structures were converted into PDBQT format using AutoDock Tools (4.2.6) with polar hydrogens added and Kollman charges assigned.[25]

Molecular docking

Molecular docking studies were performed using AutoDock 4.2.6 software downloaded by MGL Tools.[25] MGL tool is a graphical user interface (GUI) used to prepare input, run, and analyze dockings generated from AutoDock employing the Lamarckian Genetic Algorithm (LGA).[32,33] Prior to docking, ligand geometries were optimized using the MMFF94 force field to obtain energetically stable conformations. Partial atomic charges were assigned using the Gasteiger charge method, and AutoDock atom types were applied during ligand preparation in AutoDock Tools. For protein preparation, Kollman united atom charges were assigned, and polar hydrogens were added. A blind docking strategy was adopted to allow unbiased exploration of all possible binding sites.[34] The grid boxes were generated with dimensions of 70 × 70 × 70 Å to cover the entire surface of the HadAB, FabG1, and KasA protein structures, with centre coordinates fixed at (5.789, 25.971, -4.844), (9.737, 13.004, 10.860), and (-30.133, 31.931, -37.969), respectively. The rationale for employing blind docking approach is to explore all possible ligand-binding sites, whether they correspond to known sites observed in the crystal structure or represent new potential binding sites. The docking procedures included 10 runs per ligand, and the lowest binding energy conformation with maximum cluster population was selected.

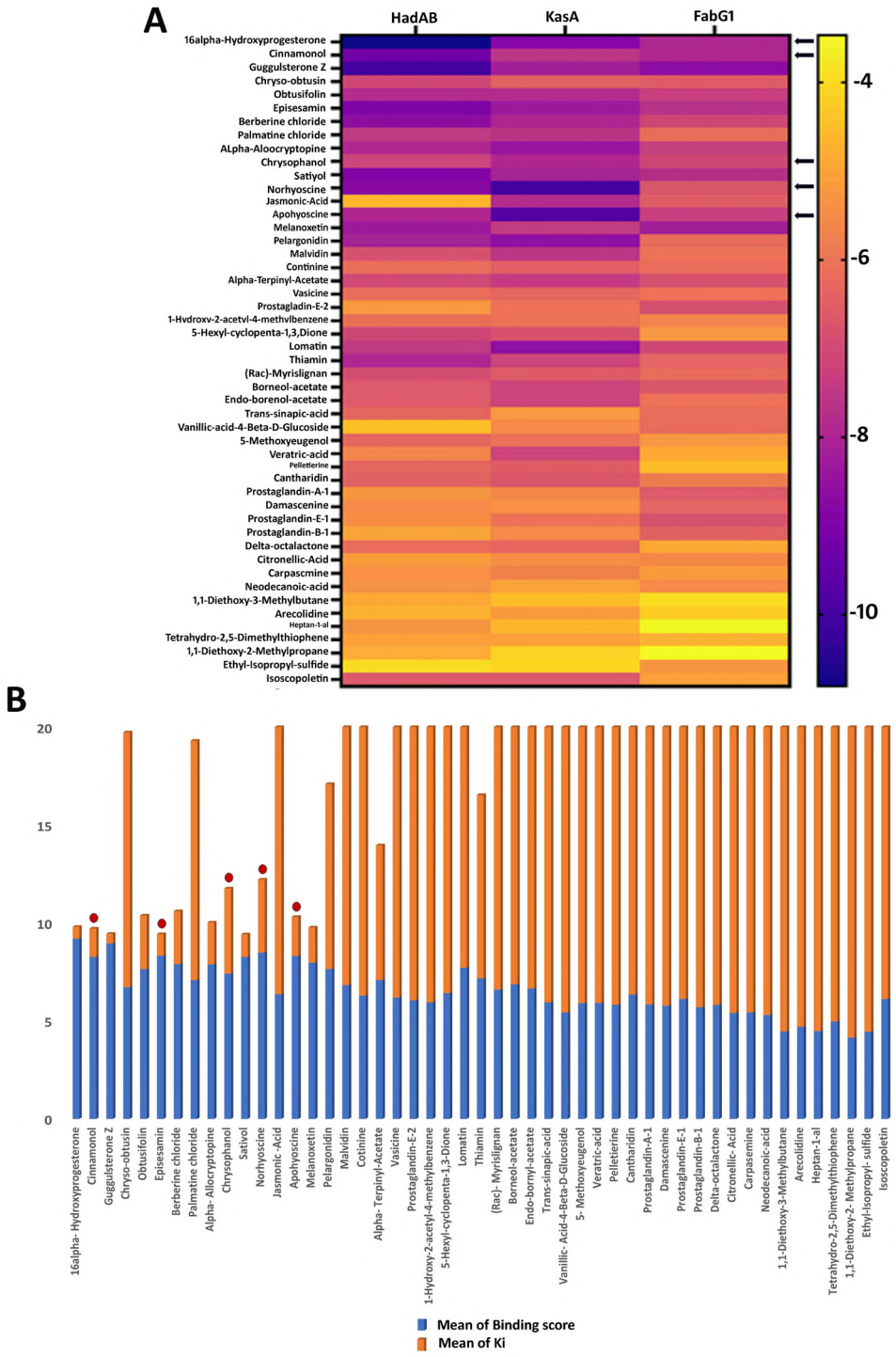

Figure 1. Molecular docking analysis of forty-nine herbal compounds against HadAB, KasA and FabG1: (A) Heatmap of the docking scores of the compounds against the three FAS-II pathway proteins. (B) Bar graph showing the average docking and inhibition scores among the three targets. The five selected lead compounds (16α-Hydroxyprogesterone, Cinnamonol, Norhyoscine, Apohyoscine and Chrysophanol) are indicated by red dots

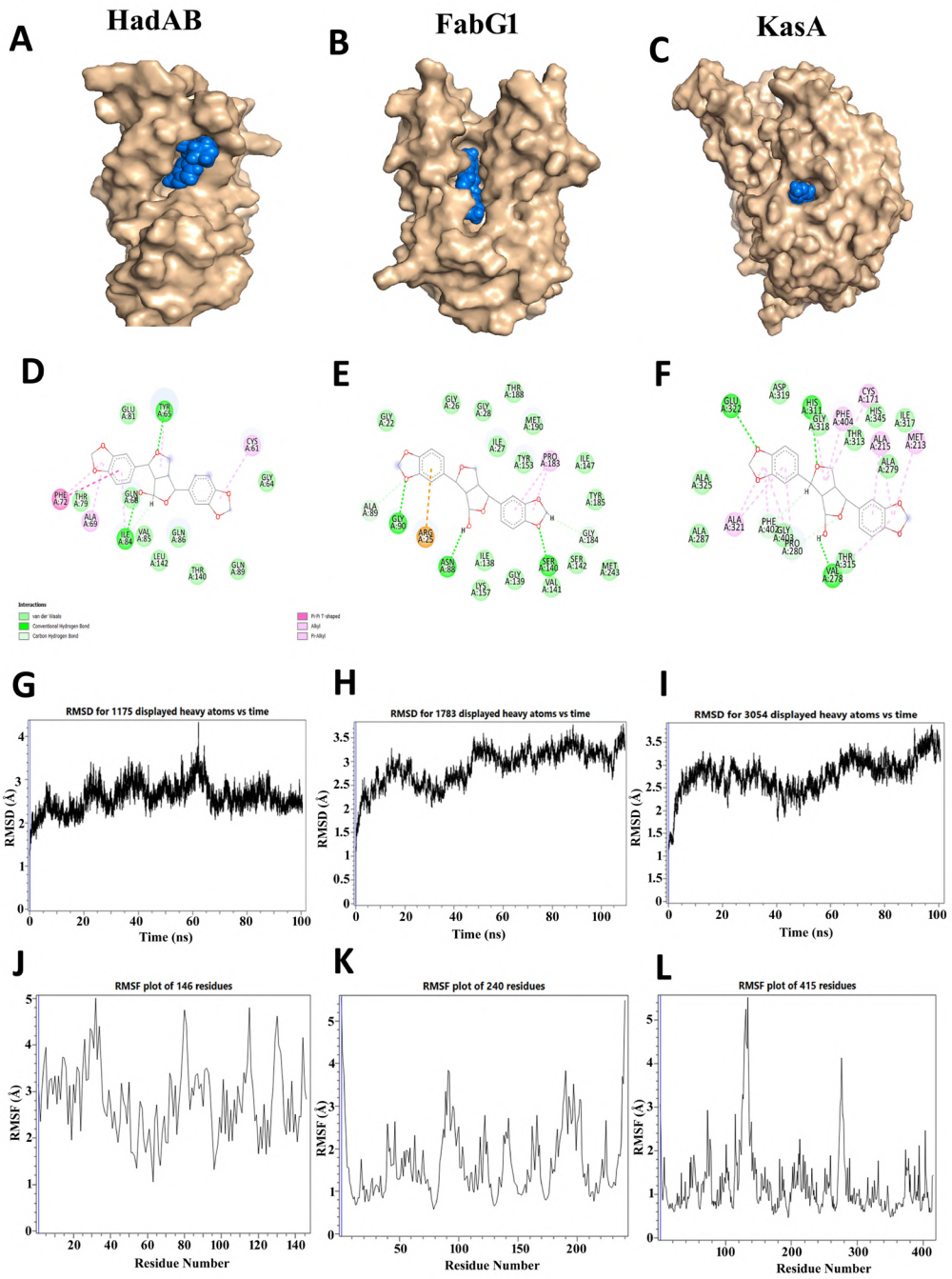

Figure 2. In silico docking study of Cinnamonol with HadAB, FabG1 and KasA proteins: (A-C) Docking poses of Cinnamonol with (A) HadAB, (B) FabG1, and (C) KasA, showing the binding pockets. (D-F) 2D interaction maps representing the interactions of Cinnamonol with respective amino acid residues. (G-I) RMSD plots of Cinnamonol-HadAB, Cinnamonol-FabG1 and Cinnamonol-KasA complexes respectively. (J-L) RMSF plots of Cinnamonol-HadAB, Cinnamonol-FabG1 and Cinnamonol-KasA complexes respectively

Binding affinity (ΔG), number of hydrogen bonds, and interaction with active site residues were key criteria for evaluating docking results. Visualization and interaction mapping were carried out using PyMOL[35] and Discovery Studio Visualizer.[36]

Molecular Dynamics (MD) simulation

To study the stability of Protein-ligand interactions predicted by molecular docking, MD simulations were performed using the Flare software suite (V.6.1, Cresset)[37] powered by the OpenMM engine. Each top-scoring protein-ligand complex was embedded in a cubic TIP3P water box with periodic boundary conditions and a 10 Å solvent padding.[38] A total of 5000 frames were saved during the simulation.

The characterization of proteins and ligands were performed by using AMBER ff14SB force field and GAFF2, respectively. The calculation of ligand partial charges was performed using the AM1-BCC method.[39] Simulations were performed under the NPT ensemble, with the system maintained at a constant temperature of 300 K and pressure of 1 atm. The integration time step was kept at 2 femtoseconds, and each production run lasted 100 ns and 50 ns, with trajectory frames being recorded every 10 picoseconds. Default Flare settings were used for other parameters, such as periodic boundary conditions, force field assignment, and handling constraints.

Trajectory analyses encompassed the calculation of RMSD (Root Mean Square Deviation), RMSF (Root-Mean-Square Fluctuation), radius of gyration (Rg), and hydrogen bond dynamics to assess the structural stability and ligand retention of the complexes.[40] Additional simulation results indicated an average radius of gyration of 17.8 Å, potential energy of -105,000 kcal/mol, density of 1.03 g/mL, and simulation box volume of 355 nm^3. These parameters have been integrated to ensure the reproducibility of the MD simulations.

Selection of lead molecules

The selection of lead compounds was based on a composite analysis of molecular docking scores, pharmacokinetic profiles, predicted toxicity, and MD simulation stability. Compounds with binding energies better than -7.0 kcal/mol, favourable ADMET properties, and minimal RMSD fluctuations (<3.0 Å) across the 100 ns and 50 ns trajectory were shortlisted. Additionally, persistence of hydrogen bonding and hydrophobic interactions with catalytic residues during the MD trajectory was considered indicative of strong and stable binding.[41] These shortlisted compounds were proposed as potential multitarget inhibitors of the FAS-II pathway for further experimental and preclinical validation.

RESULTS

Screening of *Himalayan herbs* for potential antitubercular phytochemicals

Recent studies have highlighted the pharmacological potential of *Himalayan herbs* traditionally used in *Hawan Samagri*. The present study focuses specifically on *Himalayan* plant species traditionally incorporated into *Hawan Samagri* preparations. This regional emphasis was adopted because *Himalayan* medicinal plants are known to produce unique and chemically diverse secondary metabolites as adaptive responses to ecological stressors such as high altitude, intense UV radiation, and temperature fluctuations, thereby offering a biologically enriched resource for drug discovery. From these selected herbs, forty-nine phytochemicals were systematically curated based on their documented occurrence, structural diversification, chemical diversity, pharmacological relevance, and potential volatility or persistence during fumigation (Supplementary Table 1 and Supplementary Figure 1). This curated set represents a rationally defined subset rather than the complete phytochemical repertoire of *Hawan Samagri*, ensuring both novelty and biological plausibility in the present screening approach.

Building on this, the present study identifies novel and previously unreported phytochemicals from these *Himalayan herbs* that may act as multitarget inhibitors of three key FAS-II enzymes in *M.tb* namely HadAB, FabG1, and KasA. These enzymes have been selected because they are essential, structurally conserved, and absent in humans, making them promising and underexplored targets for inhibiting mycolic acid biosynthesis in *M.tb*.[7]

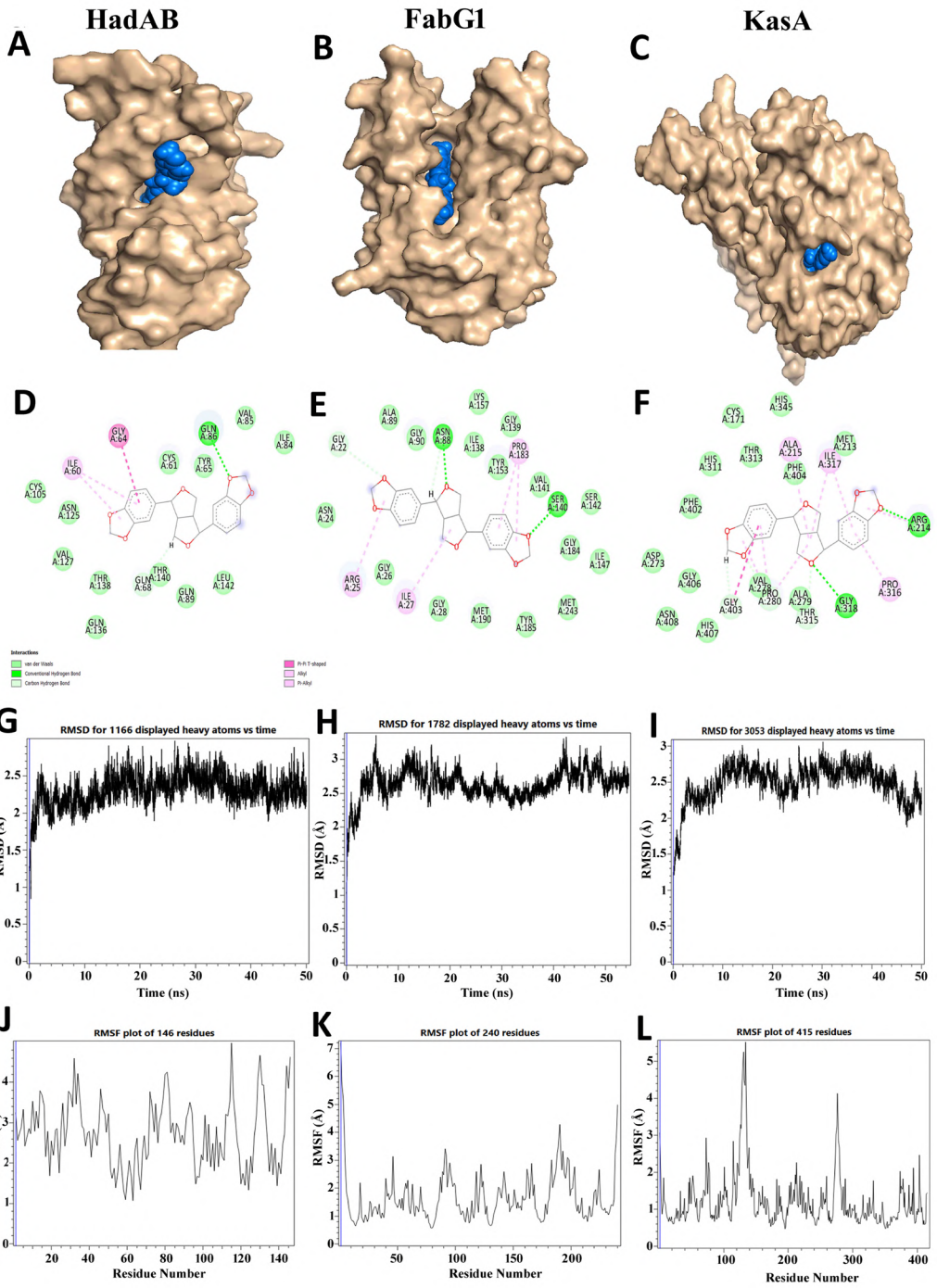

Figure 3. In silico docking analysis of Episesamin with HadAB, FabG1 and KasA proteins: (A-C) Docking poses of Episesamin with (A) HadAB, (B) FabG1 and (C) KasA with binding pockets. (D-F) 2D interaction maps of Episesamin with corresponding amino acid residues. (G-I) RMSD analyses of Episesamin-HadAB, Episesamin-FabG1 and Episesamin-KasA complexes, respectively. (J-L) RMSF profiles of the Episesamin-HadAB, Episesamin-FabG1 and Episesamin-KasA complexes, respectively

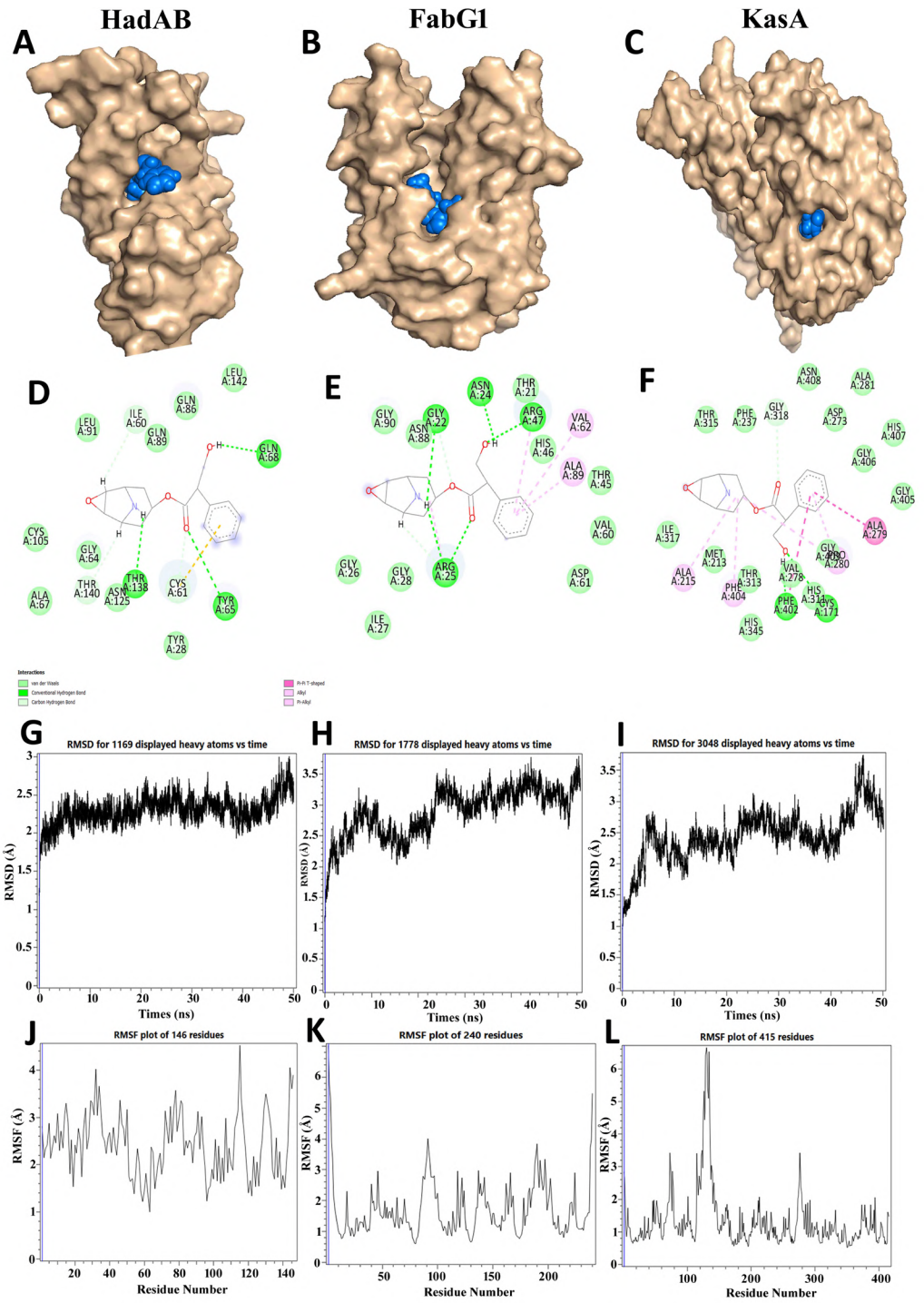

Figure 4. In silico docking analysis of Norhyoscine with HadAB, FabG1 and KasA proteins: (A-C) Docking poses of Norhyoscine with (A) HadAB, (B) FabG1 and (C) KasA. (D-F) 2D interaction maps showing the interaction of Norhyoscine with the respective amino acid residues. (G-I) RMSD analyses of the Norhyoscine-HadAB, Norhyoscine-FabG1 and Norhyoscine-KasA complexes, respectively. (J-L) RMSF profiles of Norhyoscine-HadAB, Norhyoscine-FabG1 and Norhyoscine-KasA complexes, respectively

Each selected compound had a molecular weight under 400 Da and was reported from various plant parts, including aerial parts, bark, roots, fruits, and seeds[42] (Supplementary Table 1). The focus on relatively smaller molecules was intended to enhance drug-likeness and oral bioavailability, consistent with established medicinal chemistry principles. The chemical diversity included tropane alkaloids, phenylpropanoids, lignans, and anthraquinones.[43,44] This diverse range of chemical scaffolds enhances the probability of targeting different binding environments within the enzyme active sites, thereby increasing the potential for multitarget inhibition.

Lipinski's rule of five and ADMET profiling

The screening of selected phytochemicals began with evaluating the drug-likeness and pharmacokinetic properties to ensure their suitability for oral administration and clinical progression. Lipinski's Rule of Five is a broadly accepted with criterion that helps predict oral bioavailability by assessing key physicochemical properties. Compounds that follow these rules are more likely to be absorbed and utilized effectively when administered orally.[45] Physicochemical profiling of the forty-nine selected phytochemicals was performed to evaluate their drug-likeness based on Lipinski's rule of five parameters. All compounds exhibited molecular weights below 500 Da (range: 104-387 Da), indicating favorable molecular size for oral absorption and cellular permeability. Lipophilicity assessment (XlogP3) demonstrated that the majority of compounds (46 out of 49) fell within the optimal range (-0.4 to 4.2; predominantly 1-4), reflecting a balanced hydrophilic–lipophilic profile conducive to membrane permeability. Only one compound showed slightly negative lipophilicity (Carpasemine, -0.4), suggesting higher hydrophilicity, while none exceeded the critical threshold of XlogP3 > 5, indicating minimal risk of excessive hydrophobicity-related solubility or toxicity issues.

Hydrogen-bonding capacity remained within acceptable limits for all compounds, with hydrogen bond donors ≤5 and hydrogen bond acceptors ≤10, supporting favorable membrane diffusion without compromising target-binding potential. Molar refractivity values ranged from 36.7-105.6, with the vast majority falling within the optimal range of 40-130, indicating appropriate molecular volume and polarizability for stable protein-ligand interactions.

Collectively, these findings demonstrate that the curated phytochemical library largely conforms to established drug-likeness criteria, supporting its suitability for structure-based virtual screening against FAS-II targets (Table 1 and Supplementary Table 2).

ADMET profiling is an essential part of initial drug screening that evaluates the pharmacokinetic and toxicological parameters of compounds in biological systems. This approach helps to screen drugs having high therapeutic potential and low toxicity risk, reducing costly failures in further experimental stages.[46] In silico ADMET analysis revealed that the majority of the selected phytochemicals exhibited high predicted human intestinal absorption (HIA > 90%), indicating favorable oral bioavailability (Table 1 and Supplementary Table 3). Caco-2 permeability values suggested moderate to good intestinal transport for most compounds, while MDCK permeability varied, reflecting structural diversity and differences in passive membrane diffusion. Skin permeability predictions were generally low to moderate, supporting suitability for systemic administration. Plasma protein binding (PPB) values ranged from moderate to high, with several compounds maintaining acceptable binding levels (<90%), ensuring sufficient free drug availability. Predicted BBB penetration values were mostly low to moderate, suggesting limited central nervous system exposure an advantageous feature for anti-tubercular agents. Most compounds were predicted to be non-inhibitors of CYP2D6, indicating a low risk of drug-drug interactions. Although some compounds showed predicted mutagenicity, carcinogenicity outcomes were variable and not consistently positive. Overall, the ADMET profile supports the pharmacokinetic suitability of a substantial proportion of the phytochemical library for further investigation.[47]

Molecular docking and molecular dynamics simulation analysis

Molecular docking was performed to predict the binding affinities of forty-nine phytochemicals with the target enzymes. A blind

Table 2. Binding energy, inhibition constant, and interacting amino acid of selected five lead compounds

No.	Compounds	Plant Name	HadAB B.E (kcal/mol)	Ki (μM)	Interacting A. A	FabG1 B.E (kcal/mol)	Ki (μM)	Interacting A. A	KasA B.E (kcal/mol)	Ki (μM)	Interacting A. A
1.	Cinnamonol	*Cinnamomum camphora*	-9.25	0.15	THR138, VAL127, ASN125, LEU91, ILE60, GLN89, CYS61, GLN86, ILE84, VAL85, LEU142, TYR65, GLN68, GLY64, CYS105	-7.95	1.48	GLY184, GLY90, ASN24, ARG25, GLY28, GLY26, GLY22, ASN88, ILE27, TYR153, GLY139, ILE138, SER140, PRO183	-7.59	2.72	PHE210, PRO206, LU203, ILE347, PRO201, PHE239, ILE202, GLU241, GLY200, SER346, GLU199, GLY115, LEU116
2.	Episesamin	*Commiphore mukul*	-8.96	0.27	VAL85, GLN86, LEU142, GLU68, THR140, GLY64, ILE60, CYS61, GLN89, TYR65, ILE84	-7.70	2.26	PRO238, GLY244, TRP145, VAL141, LEU144, SER140, GLY143, ILE161, VAL236, GLY246, MET245	-8.32	0.80	GLU120, GLY117, GLU199, GLY115, PHE210, ILE347, PHE404, ALA170, GLY200, PRO201, GLU203, LEU116, PRO206
3.	Norhyo-scine	*Datura metel*	-8.74	0.39	TYR39, LEU54, LEU57, ALA55, PRO56, ILE97, PRO96, LYS95, PHE93, GLU94	-6.78	10.75	ASN24, HIS46, ARG47, GLY22, ASN88, ARG25, VAL62, ASP61, VAL60, ALA89, GLY90	-9.95	0.05	PHE239, HIS345, SER346, GLU203, ILE202, GLU199, ILE347, PRO206, GLY200, GLU120, PRO201, ALA119, GLY117
4.	Apohyos-cine	*Datura metel*	-7.94	1.51	ILE97, GLN136, PRO96, PHE93, LYS95, LEU48, LEU54, TRP38, TYR39, ALA55, LEU57, PRO56	-7.30	4.42	THR191, TYR185, ILE186, ILE27, TYR153, GLY139, PRO183, GLY184, SER140, MET190, ILE147, VAL141, SER142, GLN150	-9.70	0.07	GLY117, LEU116, GLY200, SER346, PHE239, HIS345, GLU241, GLY240, ILE202, ILE347, PRO201, GLU203, PRO205, GLU199, PHE210
5.	Chryso-phanol	*Cassia tora*	-7.19	5.40	GLN86, GLN68, THR58, LEU91, ILE60, CYS61, GLN89, THR140, GLY64, ASN125	-7.11	6.14	THR191, MET190, ILE186, GLY184, GLY139, PRO183, SER140, TYR153, TYR185, ILE147, GLN150	-7.94	1.51	LEU205, LEU116, GLU199, TYR82, GLY117, GLY200, VAL83, GLU120, GLU203, PRO206

docking approach was employed to explore potential binding pockets without introducing positional bias. This strategy was particularly important to ensure unbiased identification of both canonical active site interactions and possible alternative or allosteric binding regions, thereby minimizing the risk of overlooking novel interaction sites. Such an approach is especially relevant when screening structurally diverse natural compounds, where binding preferences may not be restricted to previously characterized pockets. Supplementary Table 4 shows a summary of the docking data, which includes binding energies and inhibition constants for all compounds. To facilitate comparison of overall binding preferences, the docking scores were shown as heatmaps and bar graphs (Figures 1A and B).[7] The heatmap provides an intuitive overview of relative binding affinities, where strong binders (ΔG < -8.5 kcal/mol) are highlighted in blue, moderate binders in red, and weak binders (ΔG > -6.0 kcal/mol) in yellow (Figure 1A) allowing rapid identification of compounds with high affinity across multiple targets. The bar graph (Figure 1B) displays the average binding energies alongside their corresponding inhibition constants (Ki values) enabling a direct comparison of both binding strength and predicted potency for each compound.

Seven compounds were selected based on their binding affinities and inhibition constants: 16α-hydroxyprogesterone, guggulsterone Z, cinnamonol, norhyoscine, episesamin, apohyoscine and chrysophanol. Among them, both guggulsterone Z and 16α-Hydroxyprogesterone showed high docking affinities for all three targets in our screening (Supplementary Table 4). However, PreADMET toxicity predictions indicated potential mutagenicity and/or carcinogenicity, and their steroidal structures could interact with hormone-related pathways, limiting their suitability as lead candidates. Therefore, these compounds were excluded from further selection in the lead optimization pipeline.

The remaining five compounds were advanced for detailed analysis, as they demonstrated strong binding interactions across all three targets (Table 2). Each compound, however, showed its highest binding affinity toward a specific enzyme: Cinnamonol with HadAB (-9.25 kcal/mol), Episesamin with FabG1 (-7.70 kcal/mol), and both Norhyoscine (-9.95 kcal/mol) and Apohyoscine (-9.70 kcal/mol) with KasA. Chrysophanol, though relatively moderate, demonstrated extensive activity against all three proteins.[48]

Cinnamonol was identified as the most promising candidate among these leads due to its strong binding affinity toward HadAB (-9.25 kcal/mol), FabG1 (-7.95 kcal/mol) and KasA (-7.59 kcal/mol). In HadAB, Cinnamonol established an extensive network of interactions (Figures 2A and D), where it was stabilized by several hydrogen bonds and hydrophobic interactions. Gln68, Glu81, and Thr79 formed strong hydrogen bonds with the ligand, while van der Waals and alkyl/π-alkyl interactions strengthened binding with hydrophobic residues Leu142, Val85, Ile84, Ala69, and Phe72. Residues Cys61 and Gly64 were positioned close to the ligand, helping define the catalytic cleft. In FabG1, Cinnamonol was located near the NADH-binding site, forming interactions with Arg25, Ser140, and Asn88, while Pro183 formed π-π interactions. Additional contacts with Ala89, Gly90, and Val141 further stabilized the complex (Figures 2B and E). In KasA, the ligand was anchored within the malonyl-ACP groove and stabilized by hydrogen bonds with His311 and Glu322 (Figures 2C and F).

MD simulations over 100 ns validated stable complexation among all three enzymes, exhibiting RMSD deviations below 2.8 Å (Figures 2G-I) and RMSF fluctuations below 3.5 Å, predominantly localized in flexible loops regions (Figures 2J-L). Cinnamonol is predicted to block substrate entry into the catalytic site by occupying the hydrophobic groove of HadAB and forming stabilizing interactions, thereby inhibiting the dehydration step required for mycolic acid chain elongation.[49,50]

Episesamin, a phenylpropanoid lignan, exhibited stable binding to all three FAS-II enzymes (Figure 3). In the case of HadAB, it formed hydrogen bonds with Gln68 and Gln86, while Ile60, Gly64 and Cys61 contributed additional van der Waals contacts. Hydrophobic residues such as Leu142, Ile84, and Val85 helped keep the ligand stable in the hydrophobic cleft (Figures 3A and D). In FabG1, Episesamin firmly was positioned within

Table 3. Docking Results of Experimentally Validated Inhibitors Against Target Proteins Used for Method Validation

No.	Compounds	Plants	B. E	Ki	Interacting A. A
1.	FabG1-Isoniazid (INH)	Inhibitors	-6.85	9.52	GLY139, PRO183, ILE27, MET190, THR188, ILE186, THR191, TYR185, GLY184, VAL141, TYR153, SER140
2.	KasA-TLM	Inhibitors	-6.68	12.79	ILE207, ILE202, GLU203, PRO201, PRO206, GLY115, ILE347, GLU199, LEU116, GLY200, SER346, GLU241, PHE239
3.	KasA-Platensimycin	Inhibitors	-4.04	10.90	GLU241, ILE202, PHE239, ILE347, PRO206, PHE210, ALA119, LEU205, LEU116, GLU203, GLU120, TYR82, VAL83, GLY117, GLY118, GLU199, PRO201, GLY200
4.	HadAB-Isoxyl	Inhibitors	-7.94	1.51	THR123, ASN125, THR140, GLN68, PHE72, THR79, GLU81, ILE84, ALA69, TYR65, LEU142, GLN86, CYS61, ALA67, VAL107, CYS105, GLY64
5.	HadAB-Thioacetazone	Inhibitors	-5.82	54.16	TYR65, ILE84, GLU81, PHE72, THR79, ILE77, ALA78, LYS73, ALA69, GLN68, LEU142, GLU86, VAL85

the substrate-binding region to the area where the substrate binds, which is next to the NADH cofactor pocket (Figures 3B and E). It formed hydrogen bonds with Asn88 and Ser140 which are important for maintaining the catalytic environment. It also formed van der Waals and α-alkyl interactions with Tyr153, Pro183, Val141, and Gly139. Residues like Gly22, Arg25, and Ile27 helped stabilize the structure even more by hydrophobic and shape-complementary packing interactions (Figures 3B and E). In KasA, with hydrogen bond interactions with Arg214, and Gly318, along with hydrophobic interactions with Ala215, Ile317, Pro316, and Gly403 contributed to the stability of binding (Figures 3C and F). In conclusion, Episesamin had the strongest binding affinity with FabG1 (-7.70 kcal/mol), while HadAB (-8.74 kcal/mol) and KasA (-8.32 kcal/mol) had weaker binding affinities. The docking protocol was further validated by docking experimentally known inhibitors for each target protein under the same computational conditions. The results are presented in Table 3. The identified phytochemicals showed docking scores and binding interactions comparable to the reference inhibitors. These results support the reliability of the docking methodology and further suggest the potential of the chosen phytochemicals as potential inhibitors of HadAB, FabG1 and KasA.

Molecular dynamics simulations demonstrated that the FabG1-Episesamin complex exhibited the most stable. RMSD values stabilized after 30 ns (Figure 3G-I), and RMSF fluctuations remained below 5 Å for the majority of residues, except for minor loop motions in HadAB (Figures 3J-L). These findings collectively identify FabG1 as the principal target of Episesamin, with its direct interactions with catalytically crucial residues (Asn88 and Ser140) and neighbouring hydrophobic contacts potentially hindering β-ketoacyl intermediate positioning or obstructing NADH binding, thereby disrupting fatty acid chain elongation and subsequent mycolic acid biosynthesis.[51,52]

Norhyoscine (scopolamine) and Apohyoscine (aposcopolamine), both tropane alkaloids distinguished by their bicyclic tropane core and ester linkages, demonstrated significant affinities for all three FAS-II enzymes, with KasA identified as their principal target (-9.95 and -9.70 kcal/mol, respectively). In HadAB, Norhyoscine

formed hydrogen bonds with Tyr65, Gln68 and Thr138 and it also formed hydrophobic interactions with Gly64, Leu91, Ile60 and Leu91. Additional van der Waals contacts with Cys61 and Thr140 helped keep the binding orientation stable in a shallow pocket next to the catalytic site (Figures 4A and D). In FabG1, Norhyoscine was bound near the cofactor-binding domain where it was stabilized by forming hydrogen bonds with Asn24, Arg47, and Arg25 and hydrophobic contacts with Val60, Gly22, Gly28, Gly26, and Val60 residues (Figures 4B and E). Additional van der Waals contacts with Ala89 and Val62 helped stabilize the binding orientation in a shallow pocket next to the catalytic site. In comparison with HadAB and FabG1, Norhyoscine had the strongest binding with KasA (-9.95 kcal/mol), where it was deeply embedded in the tunnel-like substrate channel (Figures 4C and F). A strong hydrogen bond with Gly318 and hydrophobic contacts with Ala279, Val278, Gly280, and Pro373 enhanced stability. Phe402 formed π-π stacking with the ligand, which is also observed for thiolactomycin. Additional stabilization came from Ala215, Met213, Thr313, and His311, confirming its occupancy of the catalytic groove and potential to block substrate access. MD simulations demonstrated stable complex formation, with RMSD values plateauing below 3 Å and RMSF fluctuations between 4-6 Å (Figures 4J-L), confirming the conformational stability of the Norhyoscine-KasA complex.

Similarly, apohyoscine showed a similar interaction profile. HadAB was stabilized by hydrogen bonding with Gln68 and formed van der Waals and π-π stacking interactions with Thr140, Gln89, Cys61, Leu142 and Ile84 (Figures 5A and D). Apohyoscine formed hydrogen bonds with Ile27 and Gly90 in FabG1 and hydrophobic interactions with Gly26, Gly25, Val62, and Gly22, whereas additional interactions with Ala111, Leu91, Arg47, Arg25 and Ala89 improved stability at the cofactor-binding region (Figures 5B and E).

However, its highest binding affinity was observed with KasA (-9.70 kcal/mol), where the ligand occupied the same substrate tunnel as Norhyoscine (Figures 5C and F). Strong π-π stacking with Phe402 and Phe404, and hydrophobic interactions involving Gly403, Gly318, Gly405, and Gly406 formed an extensive interaction network. The broader contact surface compared to Norhyoscine suggests improved stability and tighter binding. MD simulations corroborated this, demonstrating RMSD stabilization after 25 ns (Figure 5G-I) and uniform RMSF values across catalytic residues (Figure 5J-L).

In general, both alkaloids had stable but different affinities for all three enzymes. They bound moderately to HadAB and FabG1 and strongly to KasA. Their occupation of the substrate channel and π-π stacking with Phe402, a conserved residue in known inhibitors, supports their role as competitive blockers of the condensation step in mycolic acid chain elongation, thereby disrupting the FAS-II pathway.

Chrysophanol, an anthraquinone derivative previously documented for its antimycobacterial efficacy (MICs of 64 µg/mL against *M.tb* H37Ra and 64-128 µg/mL against *M. bovis*), demonstrated extensive yet moderate binding across HadAB, FabG1, and KasA (Figures 6A-C).

Unlike the other ligands that exhibited target preference, Chrysophanol maintained consistent interaction patterns with all three enzymes.

In HadAB, Chrysophanol formed hydrogen bonds with Gln68 and Gln86, which were further strengthened by hydrophobic interactions with Cys61, Ile60, and Gln89 (Figures 6A and D). In FabG1, the ligand formed hydrogen bonds with Asn24 and Val60. It also formed van der Waals and π-π stacking interactions with Val62, Ala111, Ala89, and Arg25, which could disrupt cofactor stabilization near the NADH-binding pocket (Figure 6B and E). In KasA, Chrysophanol was found in the substrate tunnel, where it formed hydrogen-bond interactions with Asp273 and Val278 and strong π-π stacking interactions with Phe402, Phe404, His311. It was further stabilized by hydrophobic contacts with Gly403, Gly406, Cys171 and Ala279 (Figures 6C and F).

MD simulations confirmed stable binding in all three protein-ligand complexes, with RMSD convergence occurring between 5-35 (Figure 6G-I) ns and RMSF values typically below 6 Å, suggesting restricted flexibility in critical active-site regions (Figures 6J-L). Comprehensive analyses of temperature, velocity, potential energy, density gradient, box volume, and radius of gyration for all five selected compounds in relation to HadAB,

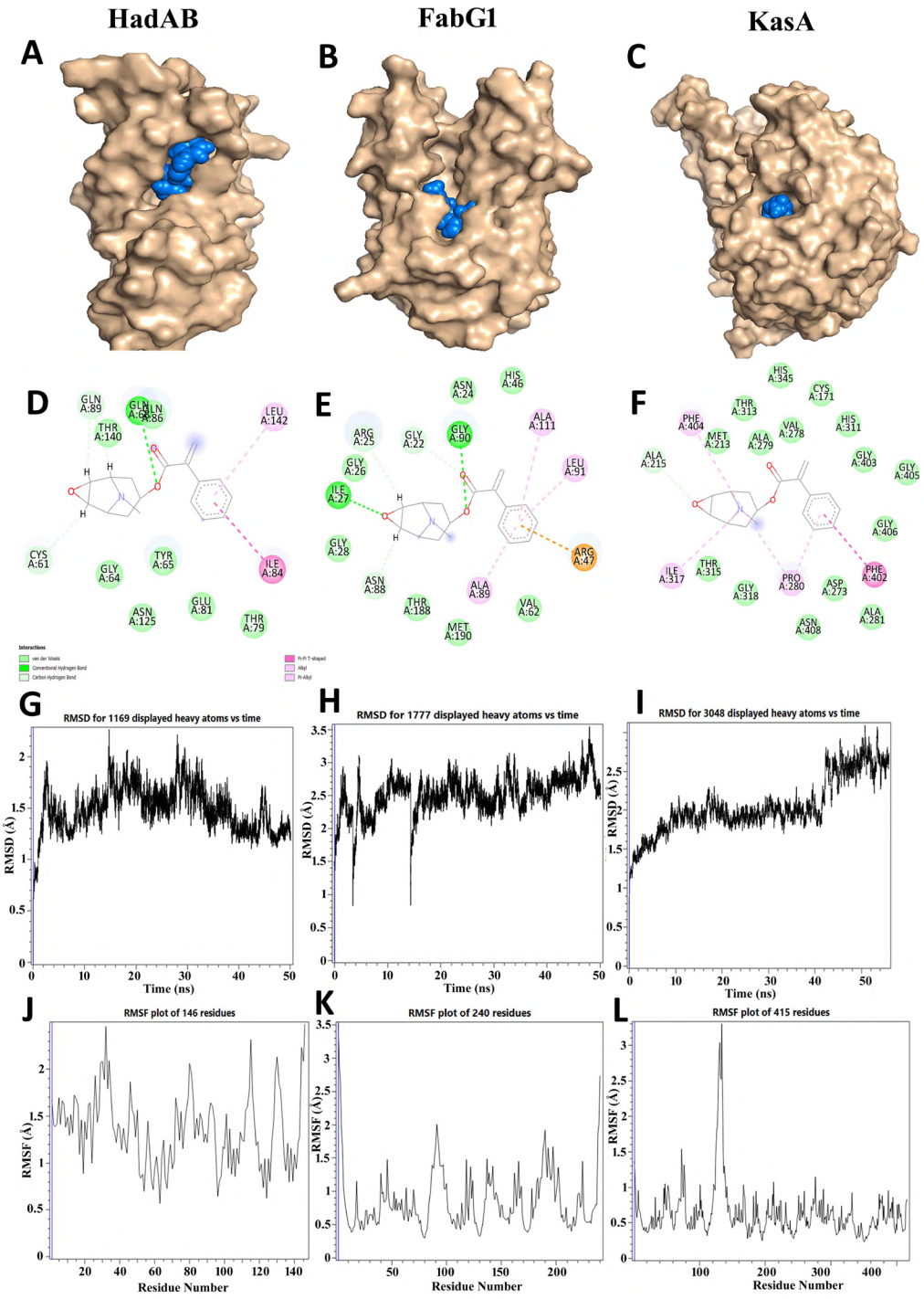

Figure 5. In silico docking analysis of Apohyoscine with HadAB, FabG1, and KasA proteins: (A-C) Docking poses of Apohyoscine with (A) HadAB, (B) FabG1, and (C) KasA. (D-F) 2D interaction maps showing the interactions of Apohyoscine with the corresponding amino acid residues. (G-I) RMSD analyses of the Apohyoscine-HadAB, Apohyoscine-FabG1, and Apohyoscine-KasA complexes, respectively. (J-L) RMSF profiles of the Apohyoscine-HadAB, Apohyoscine-FabG1, and Apohyoscine-KasA complexes, respectively

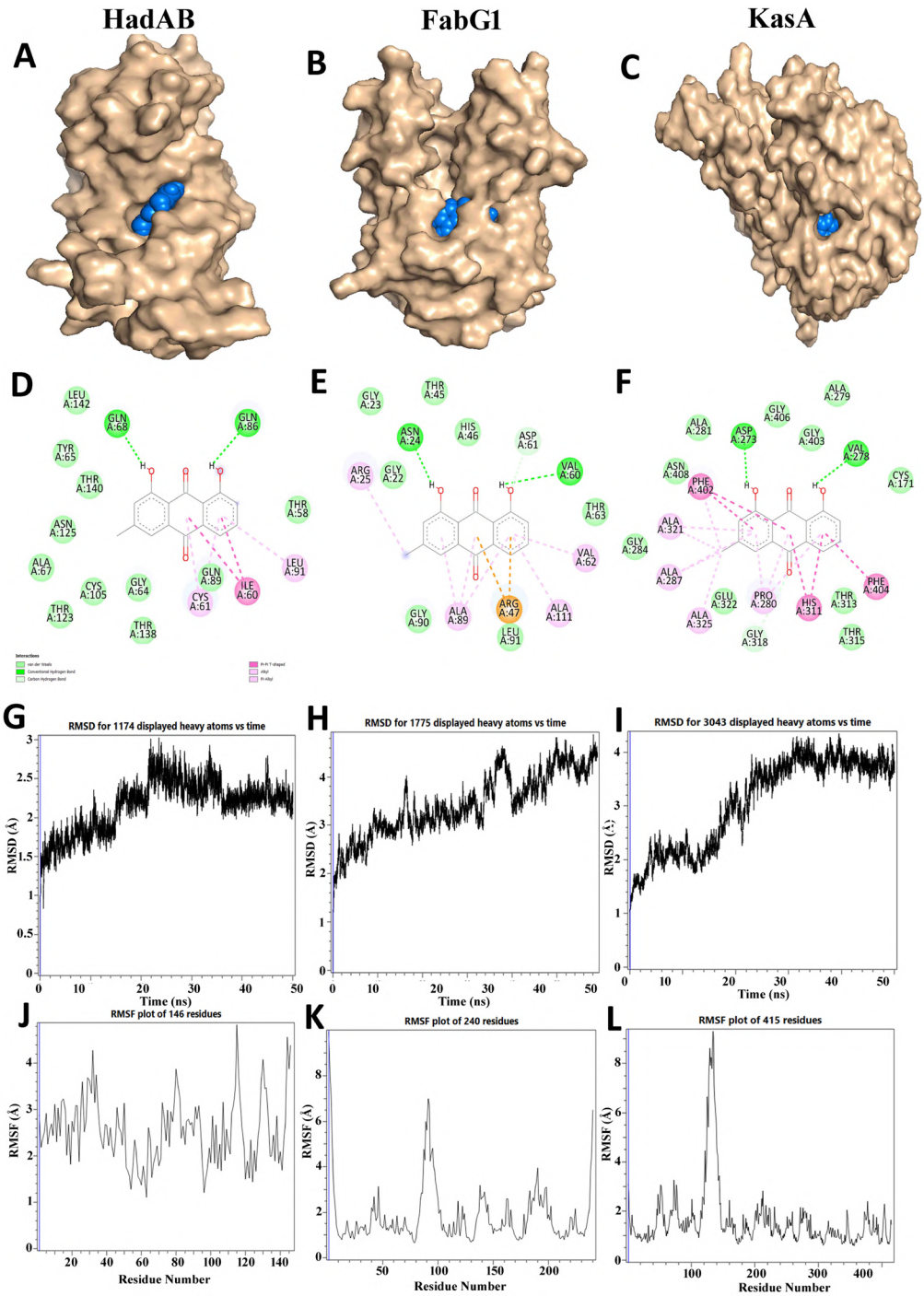

Figure 6. In silico docking analysis of Chrysophanol with HadAB, FabG1, and KasA proteins: (A-C) Docking poses of Chrysophanol with (A) HadAB, (B) FabG1, and (C) KasA, showing the binding pockets. (D-F) 2D interaction maps showing the interactions of Chrysophanol with the corresponding amino acid residues. (G-I) RMSD analyses of the Chrysophanol-HadAB, Chrysophanol-FabG1, and Chrysophanol-KasA complexes, respectively. (J-L) RMSF profiles of the Chrysophanol-HadAB, Chrysophanol-FabG1, and Chrysophanol-KasA complexes, respectively

FabG1, and KasA are illustrated in Supplementary Figures 2, 3, and 4, respectively. Chrysophanol's ability to consistently block multiple targets shows that it could be a broad-spectrum inhibitor that can block substrate access and interfere with multiple steps.

All five selected phytocompounds Cinnamonol, Norhyoscine, Episesamin, Apohyoscine, and Chrysophanol, were found to bind directly within or next to the substrate-binding pockets of HadAB, FabG1, and KasA. These pockets are normally occupied by other intermediates or cofactors, like β-hydroxyacyl-ACP, NADH, and malonyl-ACP. It is predicted that these phytochemicals compete for the binding pockets and block substrate entry, thereby either slowing down or completely inhibiting with the FAS-II pathway. This inhibition process compromises mycolic acid synthesis, an essential component of the mycobacterial cell wall, ultimately weakening the cell wall structure and leading to the bacterial cell death. The ability of these compounds to bind to multiple targets makes them more likely to be tested further as broad-spectrum FAS-II inhibitors.

Binding site analysis and inhibition mechanism

Comparison with reference inhibitors reinforced the predicted mechanisms. Cinnamonol and Norhyoscine were found to bind near the KasA malonyl-ACP tunnel. In HadAB, Cinnamonol occupied a hydrophobic cleft similar to the binding region of thiolactomycin. In FabG1, Cinnamonol and Episesamin occupied residues surrounding the NADH cofactor pocket, resembling NADH-mimetic inhibitors reported in similar systems. These findings suggested that FAS-II enzymes are likely inhibited through a competitive mechanism, targeting multiple steps of mycolic acid biosynthesis and ultimately weakening the structural integrity of the *M.tb* cell wall.[17]

DISCUSSION

The present study provides new insights into the potential of *Himalayan herb*-derived phytochemicals as multitarget inhibitors of the FAS-II pathway in *M.tb*. With the persistent global rise of MDR and XDR TB strains,[53] it is increasingly important to identify new chemical scaffolds that can act on underexplored yet essential enzymes such as HadAB, FabG1, and KasA.[54] In contrast to InhA, the traditional target of first-line *M.tb* drugs, which is susceptible to resistance-inducing mutations in *katG* or *InhA* itself, these enzymes maintain structural conservation and are indispensable, rendering them logical drug targets for next-generation anti-TB therapeutics. In this context, *Hawan Samagri*, a traditional Ayurvedic polyherbal mixture made up of different *Himalayan herbs* served as a source of bioactive phytochemicals that helped us identify possible FAS-II inhibitors.

Among forty-nine selected phytochemicals, five compounds, namely Cinnamonol, Episesamin, Norhyoscine, Apohyoscine and Chrysophanol were selected as lead compounds due to their high binding affinities and stable interactions during MD simulations. Notably, Cinnamonol has been reported previously as an antimicrobial agent, having activity against *Staphylococcus aureus* and *Candida albicans,*[55] while Chrysophanol has been established as an antimycobacterial agent showing activity against *M.tb* H37Ra and *M. bovis.*[44] This discovery expands the known range of phytochemicals with anti-TB potential.[54] On the other hand, Episesamin, Norhyoscine, and Apohyoscine have not been previously reported to have antimicrobial or antitubercular activity in the literature. Therefore, their discovery in this work as potential FAS-II enzyme inhibitors represents a novel contribution.

Previous research on natural FAS-II inhibitors has mostly focused on fatty acid mimetics, β-ketoacyl analogs, or thiolactone derivatives like cerulenin and thiolactomycin. However, the discovery of phenylpropanoids and lignans such as Cinnamonol and Episesamin in the current investigation indicates a structurally unique class of inhibitors with potential for increased bioavailability and lower toxicity. This emphasizes phytochemical diversity as an underexplored pool of anti-TB leads and underlines the case for screening traditional herbal formulations such as *Hawan Samagri* for drug development.

The identified phytochemicals were also compared with established FAS-II inhibitors such as thiolactomycin, cerulenin, platensimycin, and GSK3011724A. Cinnamonol demonstrated strong

and consistent binding across HadAB, FabG1, and KasA, with interaction energies comparable to or better than those of thiolactomycin and cerulenin. Its predicted binding pockets overlapped with critical residues such as Phe402 and Gly318 in KasA and Glu199 and Leu185 in HadAB, which are known to interact with reference inhibitors, suggesting a conserved mechanism of action.

Besides having high binding affinity against all three FAS-II enzymes, all these compounds also possess high affinity for individual targets. For example, Cinnamonol shows high binding affinity for HadAB, Episesamin for FabG1, and both Norhyoscine and Apohyoscine for KasA enzyme. The result of molecular docking suggested that Episesamin stably binds within the NADH-binding site of FabG1, highlighting its cofactor-competition mode of action.[7] On the other hand, Norhyoscine and Apohyoscine occupied the substrate channel of KasA where they both interact with Phe402 and Gly318 residues, which form the catalytic core of the enzyme. These residues have been previously reported to be the binding targets of Known inhibitors such as platensimycin and GSK3011724A, suggesting the plausibility of our docking methods.

The most promising inhibitor identified in this study was Cinnamonol.[17] It showed strong binding affinity against all three FAS-II pathway enzymes, suggesting that it can be utilized as a multitarget inhibitor to inhibit mycolic acid synthesis. Although its predicted binding sites are similar to those of known inhibitors such as cerulenin and thiolactomycin, Cinnamonol showed better pharmacokinetic properties and higher stability compared to these synthetic inhibitors. Similarly, Chrysophanol showed a wide binding affinity range as well as high binding affinity for all three FAS-II enzymes, supporting its previously reported antimycobacterial activity and making it a suitable option for combination therapy.[56]

Overall, this study achieves two major objectives: (i) it supports traditional claims and identifies new scaffolds for future drug development. This is achieved by identifying compounds with known antimicrobial activity such as Cinnamonol and Chrysophanol, and (ii) It identifies novel scaffolds for future drug development by characterizing compounds with no prior information on antibacterial activity, including Episesamin, Norhyoscine and Apohyoscine.[57-59]

CONCLUSION

This study identified five phytochemicals-Cinnamonol, Episesamin, Norhyoscine, Apohyoscine, and Chrysophanol as promising multitarget inhibitors of *M.tb* FAS-II enzymes HadAB, KasA, and FabG1. All compounds demonstrated high affinities, stable interactions, as well as favorable pharmacokinetic profiles using an integrated docking pipeline, ADMET screening, and molecular dynamics simulations. Cinnamonol bound to all three enzymes with high affinity, indicating its potential as a multitarget inhibitor. The anticipated interactions indicate the successful suppression of mycolic acid biosynthesis, a crucial process for *M.tb* survival. These studies suggest that experimental validation should include enzyme assays, inhibitor concentration evaluations, and in vitro antimycobacterial studies. In general, ethnomedicinal phytochemicals could be used to develop novel antitubercular drugs.

Future perspectives and limitations

The current study offers novel insights into the potential of Cinnamonol and other analogous herbal scaffolds as FAS-II inhibitors; however, several limitations persist. The predictions are derived from in silico analyses, necessitating in vitro as well as in vivo validation to ascertain biological efficacy together with target specificity. Future research should concentrate on lead optimization via structure–activity relationship analyses to improve binding affinity and pharmacokinetic characteristics. Additionally, toxicity and cytocompatibility evaluations are crucial for assessing safety profiles prior to preclinical testing. Combining these experimental validations will confirm the computational results and help advance phytochemical-based antitubercular drug development.

SUPPLEMENTARY INFORMATION

Supplementary information accompanies this article at https://doi.org/10.22207/JPAM.20.3.57

Additional file: Tables S1-S4 and Figures S1-S4.

ACKNOWLEDGMENTS

The authors thank the members of the Research Committee, Department of Biological Sciences and Biotechnology, Chhatrapati Shahu Ji Maharaj University, Kanpur, Uttar Pradesh, India, for their constructive feedback and thoughtful suggestions, which greatly enhanced the depth of this study.

CONFLICT OF INTEREST

The authors declare that there is no conflict of interest.

AUTHORS' CONTRIBUTION

JS, DKV, and RS conceptualized the study. JS, DKV, and RS contributed to the methodology. JS, KS, VV, DKV, and RS performed the investigation. JS, KS, and DKV contributed to data curation. JS and DKV contributed to visualisation and wrote, reviewed, and edited the manuscript. DKV supervised the study. All authors read and approved the final manuscript for publication.

FUNDING

This research was funded by Chhatrapati Shahu Ji Maharaj University, Kanpur, and the Anusandhan National Research Foundation (ANRF) under the Prime Minister's Early Career Research Grant Scheme, through the Large Research Group Project (Grant/File No.: ANRF/ECRG/2024/006549/LS).

DATA AVAILABILITY

All datasets generated or analyzed during this study are included in the manuscript and/or in the supplementary files.

ETHICS STATEMENT

Not applicable.

REFERENCES

1. Zhang M, Tian Y, Gao B, et al. Interpretation of the Global Tuberculosis Report 2025: Global epidemic trends and China's control strategy. *Zoonoses*. 2026;18;6(1):994. doi: 10.15212/ZOONOSES-2026-0002
2. Goletti D, Meintjes G, Andrade BB, Zumla A, Lee SS. Insights from the 2024 WHO global tuberculosis report–more comprehensive action, innovation, and investments required for achieving WHO end TB goals. *International Journal of Infectious Diseases*. 2025;1;150. doi: 10.15212/ZOONOSES-2024-0061
3. Adesola RO, Adebowale EA. *Mycobacterium tuberculosis*: mechanisms and interactions between drug resistance mutations with fitness costs and drug resistance phenotypes. *Infect Dis Trop Med.* 2022;8:e1044. Doi: 10.32113/idtm_202212_1044
4. Arunachalam K, Sasidharan SP, Arunachalam K, Sasidharan SP. Molecular Docking Methods for Drug Design. In: *Bioassays in Experimental and Preclinical Pharmacology.* Springer Protocols Handbooks. Humana, New York, NY. 2021;259- 262. doi: 10.1007/978-1-0716-1233-0_24
5. Bandhoria P, Gupta B, Gupta K. Crystal structure of guggulsterone Z. *Crystallogr Rep.* 2006;51:265-270. doi: 10.1134/S106377450602012X
6. Bibens L, Becker JP, Dassonville-Klimpt A, Sonnet P. A review of fatty acid biosynthesis enzyme inhibitors as promising antimicrobial drugs. *Pharmaceuticals*. 2023;16(3):425. doi: 10.3390/ph16030425
7. BIOVIA DS. BIOVIA Discovery Studio Visualizer. Software version 20. 2017;779.
8. Biswas R, Dutta A, Dutta D, et al. Crystal structure of dehydratase component HadAB complex of mycobacterial FAS-II pathway. *Biochem Biophys Res Commun.* 2015;458(2):369-74. doi: 10.1016/j.bbrc.2015.01.119
9. Harrison GA, Wang ER, Cho K, et al. Inducing vulnerability to InhA inhibition restores isoniazid susceptibility in drug-resistant *Mycobacterium tuberculosis*. *Mbio.* 2024;13;15(3):e02968-23. doi: 10.1128/mbio.02968-23
10. Cohen-Gonsaud M, Ducasse S, Hoh F, Zerbib D, Labesse G, Quemard A. Crystal Structure of MabA from Mycobacterium tuberculosis, a Reductase involved in Long-chain Fatty Acid Biosynthesis. *J Mol Biol*. 2002;320(2):249-261. doi: 10.1016/s0022-2836(02)00463-1
11. De Silva SL. Differentiating between forms of *Mycobacterium tuberculosis* disease through immune markers. [PhD thesis], Monash University. 2018.
12. Dias DA, Urban S, Roessner U. A historical overview of natural products in drug discovery. *Metabolites.* 2012;2(2):303-336. doi: 10.3390/metabo2020303
13. Dong Y, Qiu X, Shaw N, et al. Molecular basis for the inhibition of β-hydroxyacyl-ACP dehydratase HadAB complex from *Mycobacterium tuberculosis* by flavonoid inhibitors. *Protein Cell.* 2015;6(7):504-517. doi: 10.1007/s13238-015-0181-1
14. Dookie N, Rambaran S, Padayatchi N, Mahomed S, Naidoo K. Evolution of drug resistance in *Mycobacterium tuberculosis*: a review on the molecular determinants of resistance and implications for personalized care. *J Antimicrob Chemother.* 2018;73(5):1138-1151. doi: 10.1093/jac/dkx506

15. Duan X, Xiang X, Xie J. Crucial components of mycobacterium type II fatty acid biosynthesis (Fas-II) and their inhibitors. *FEMS Microbiol Lett.* 2014;360(2):87-99. doi: 10.1111/1574-6968.12597
16. Dulsat J, Lopez-Nieto B, Estrada-Tejedor R, Borrell JI. Evaluation of Free Online ADMET Tools for Academic or Small Biotech Environments. *Molecules.* 2023;28(2):776. doi: 10.3390/molecules28020776
17. Duran-Iturbide NA, Diaz-Eufracio BI, Medina-Franco JL. In silico ADME/Tox profiling of natural products. *ACS Omega.* 2020;5(26):16076-16084. doi: 10.1021/acsomega.0c01581
18. Dutta D, Bhattacharyya S, Roychowdhury A, Biswas R, Das AK. In Silico ADME/Tox Profiling of Natural Products: A Focus on BIOFACQUIM. *Biochem J.* 2013;450(1):127-139. doi: 10.1042/BJ20121107
19. Eastman P, Swails J, Chodera JD, et al. OpenMM 7: high performance molecular dynamics. *PLoS Comput Biol.* 2017;13(7):e1005659. doi: 10.1371/journal.pcbi.1005659
20. Faion L, Djaout K, Frita R, et al. Discovery of the first *Mycobacterium tuberculosis* MabA (FabG1) inhibitors through a fragment-based screening. *Eur J Med Chem.* 2020;200:112440. doi: 10.1016/j.ejmech.2020.112440
21. Forli S, Huey R, Pique ME, Sanner MF, Goodsell DS, Olson AJ. AutoDock suite for virtual drug screening. *Nat Protoc.* 2016;11(5):905-919. doi: 10.1038/nprot.2016.051
22. Gorinova N, Atanassov A, Velcheva M. Physochlaina Species: In Vitro Culture and the Production of Physochlaine and Other Tropane Alkaloids. In: Bajaj YPS, eds. *Medicinal and Aromatic Plants XI. Biotechnology in Agriculture and Forestry,* vol 43. Springer, Berlin, Heidelberg; 1999:350-363. doi: 10.1007/978-3-662-08614-8_21
23. Holland HL. Recent advances in applied and mechanistic aspects of the enzymatic hydroxylation of steroids by whole-cell biocatalysts. *Steroids.* 1999;64:178–86. doi: 10.1016/S0039-128X(98)00085-3
24. Hurmath Unnissa S. Molecular modeling and synthesis of analogs as antitubercular agents. [PhD thesis]. Tamilnadu Dr. MGR Medical University. 2016.
25. Jayabal D, Jayanthi S, Thirumalaisamy R, Karthika R, Iqbal MN. Comparative anti-Diabetic potential of phytocompounds from Dr. Duke's phytochemical and ethnobotanical database and standard antidiabetic drugs against diabetes hyperglycemic target proteins: an in silico validation. *J Biomol Struct Dyn.* 2023;41(24):1513715149. doi: 10.1080/07391102.2023.2187231
26. North EJ, Jackson M, Lee RE. Targeting mycolic acid biosynthesis for TB therapy. *Curr Pharm Des.* 2014;20(27):4357-4378. doi: 10.2174/1381612819666133118203641
27. Jejurikar BL, Rohane SH. Drug designing in Discovery Studio. *Asian Journal of Research in Chemistry*. 2021;14(2):135-138. doi:10.5958/0974-4150.2021.00025.0
28. Kapilashrami K, Bommineni Gopal R, Machutta CarlA, et al. Thiolactomycin-based B-Ketoacyl-ACPM synthase A (KASA) inhibitors. *J Biol Chem*. 2013;288(9):6045-6052. doi: 10.1074/jbc.m112.414516
29. Dong Y, Qiu X, Shaw N, Xu Y, Sun Y, Li X, Li J, Rao Z. Molecular basis for the inhibition of β-hydroxyacyl-ACP dehydratase HadAB complex from Mycobacterium tuberculosis by flavonoid inhibitors. *Protein & cell.* 2015;6(7):504-17. doi: 10.1007/s13238-015-0181-1
30. Cohen-Gonsaud M, Ducasse S, Hoh F, Zerbib D, Labesse G, Quemard A. Crystal structure of MabA from Mycobacterium tuberculosis, a reductase involved in long-chain fatty acid biosynthesis. *J Mol Biol*. 2002;320(2):249-61. doi: 10.1016/S0022-2836(02)00463-1
31. Kuang W, Zhang H, Wang X, Yang P. Overcoming *Mycobacterium tuberculosis* through small molecule inhibitors to break down cell wall synthesis. *Acta Pharm Sin B.* 2022;12(8):3201–14. doi: 10.1016/j.apsb.2022.04.014
32. Kuo YH, Chen WC, Lin YT. Chemistry of cineole tree leaf extractives. *J Chin Chem Soc.* 1984;31(2):159-163. doi: 10.1002/jccs.198400021
33. Lakshminarayana SB, Huat TB, Ho PC, et al. Comprehensive physicochemical, pharmacokinetic and activity profiling of anti-TB agents. *J Antimicrob Chemother.* 2014;70(3):857-867. doi: 10.1093/jac/dku457
34. Lee H, Kim J, Kim J, Park YJ. Review of the global burden of tuberculosis in 2023: insights from the WHO Global Tuberculosis Report 2024. *Public Health Wkly Rep*. 2025;18(11 Suppl):55. doi: 10.56786/PHWR.2025.18.11suppl.5
35. Lipinski CA. Lead- and drug-like compounds: the rule-of-five revolution. *Drug Discov Today Technol.* 2004;1(14):337-341. doi: 10.1016/j.ddtec.2004.11.007
36. Mahanta S, Gogoi B, Tanti B. Analytics for In Silico Development of Inhibitors from Neem (*Azadirachta Indica*) Against Pantothenate Synthetase of *Mycobacterium Tuberculosis*. In: Sharma N, Chakrabarti A, Balas VE, Martinovic J, eds. *Data Management, Analytics and Innovation. Advances in Intelligent Systems and Computing*, vol 1175. Springer, Singapore. 2021:179-200. doi: 10.1007/978-981-15-5619-7_11
37. Morris GM, Goodsell DS, Halliday RS, et al. Automated docking using Lamarckian GA. *J Comput Chem.* 1998;19(14):1639-1666. doi: 10.1002/(SICI)1096-987X(19981115)19:14<1639::AID-JCC10>3.0.CO;2-B
38. Morris GM, Goodsell DS, Huey R, Olson AJ. Distributed automated docking of flexible ligands to proteins: Parallel applications of AutoDock 2.4. *J Comput Aided Mol Des.* 1996;10:293-304. doi: 10.1007/BF00124499
39. Mustafa NF, Cheng KK, Razali SA, Nadri MH. Molecular Docking and Pharmacokinetics Analysis of Phytochemicals from Piper caninum as Dengue NS2B-NS3 Protease Inhibitors. *J Trop Life Sci.* 2024;14:131–42. doi: 10.11594/jtls.14.01.14
40. Nakayama Y, Kaneko H. Development of New Molecular Descriptors Based on Flare Software Considering Three-Dimensional Chemical Structures. *Ind Eng Chem Res.* 2023;63(1):49-55. doi: 10.1021/acs.iecr.3c02775
41. Nandi S, Saxena AK. Exploring Targets of Cell Wall Protein Synthesis and Overexpression Mediated Drug Resistance for the Discovery of Potential M. tb Inhibitors. *Curr Top Med Chem.* 2021;21(21):1922-42.

doi: 10.2174/1568026621666210727165742
42. do Nascimento MLLB, de Sá Guimarães Nolêto IR, Torres-Leal FL, da Silva FCC, de Castro e Sousa JM. Cellular toxicity of organotellurans: a systematic review of pre-clinical studies. *Naunyn-Schmiedeberg's Arch Pharmacol*. 2025; 398(11):14589-14601. doi: 10.1007/s00210-025-04249-x
43. World Health Organization (WHO). Consolidated guidance on tuberculosis data generation and use. Module 1. Tuberculosis surveillance. 2024. https://www.who.int/publications/i/item/9789240075290
44. Prateeksha, Yusuf MA, Singh BN, et al. Chrysophanol: A Natural Anthraquinone with Multifaceted Biotherapeutic Potential. *Biomolecules*. 2019;9(2):68. doi: 10.3390/biom9020068
45. Pushkala VP. A comprehensive review on in silico computational studies of Siddha formulations against SARS - CoV- 2. CABI Databases. https://www.cabidigitallibrary.org/doi/pdf/10.5555/20220167831
46. Rastogi V, Krishnanand S, Panwar RB, et al. Quality analysis and antibacterial activity of ethnobotanical fumes. *Interdiscip J Yagya Res.* 2022;5(1):1-19. doi: 10.36018/ijyr.v5i1.79
47. Rastogi V, Tomar J, Patni T, Vijay C, Sharma P. Anti tubercular minimum inhibitory concentration (MIC) and chemical characterization of ethnobotanical mixture used in the treatment of tuberculosis. *Indian J Microbiol Res*. 2019;6(1):50-56. doi: 10.18231/2394-5478.2019.0011
48. Rudraraju RS, Daher SS, Gallardo-Macias R, Wang X, Neiditch MB, Freundlich JS. *Mycobacterium tuberculosis* KasA as a drug target: Structure-based inhibitor design. *Front Cell Infect Microbiol.* 2022;12:1008213. doi: 10.3389/fcimb.2022.1008213
49. Sairkar P, Sharma A, Shukla N. Estimation of guggulsterone E and Z in the Guggul-based commercial formulations using high-performance thin-layer chromatography. *J Pharm Bioallied Sci*. 2017;9(1):1. doi: 10.4103/0975-7406.206225
50. Schiebel J, Kapilashrami K, Fekete A, et al. Structural Basis for the Recognition of Mycolic Acid Precursors by KasA, a Condensing Enzyme and Drug Target from *Mycobacterium Tuberculosis*. *J Biol Chem.* 2013;288(47):34190-34204. doi: 10.1074/jbc.m113.511436
51. Sharma A, Islam MH, Fatima N, et al. Elucidation of marine fungi derived anthraquinones as mycobacterial mycolic acid synthesis inhibitors: an in silico approach. *Mol Biol Rep.* 2019;46(2):1715–25. doi: 10.1007/s11033-019-04621-0
52. Shimizu S, Akimoto K, Shinmen Y, Kawashima H, Sugano M, Yamada H. Sesamin is a potent and specific inhibitor of Δ5 desaturase in polyunsaturated fatty acid biosynthesis. *Lipids.* 1991;26(7):512-516. doi: 10.1007/BF02536595
53. Shinde R, Suvarna V. Fatty Acid Biosynthesis: An Updated Review on KAS Inhibitors. *Curr Drug Discov Technol.* 2022;19(2):1-15. doi: 10.2174/1570163819666220111113032
54. Stelitano G, Cocorullo M, Chiarelli LR. Multi-target Compounds for Tuberculosis. In: Peters J, eds. *Polypharmacology: Strategies for Multi-Target Drug Discovery*. 2025:437-49. doi: 10.1002/9781394182862.ch28
55. Xie L, Tang H, Song J, Long J, Zhang L, Li X. Chrysophanol: a review of its pharmacology, toxicity and pharmacokinetics. *Journal of Pharmacy and Pharmacology*. 2019;71(10):1475-87. doi: 10.1111/jphp.13143
56. Perez GRM. Anti-inflammatory activity of compounds isolated from plants. *The Scientific World Journal.* 2001;1(2):713-84. doi: 10.1100/tsw.2001.77
57. Tripathi PK, Jain CK. Computational drug discovery against *Acinetobacter baumannii. J Mater Sci Surf Eng.* 2019;6(6):895-898. doi: 10.jmsse/2348-8956/6-6.4
58. Umar HI, Ajayi A, Bello RO, et al. Novel molecules derived from 3-O-(6-galloylglucoside) inhibit main protease of SARS-CoV 2 in silico. *Chem Pa.* 2022;76(2):785-796. doi: 10.1007/s11696-021-01899-y
59. Vasconcelos NG, Croda J, Simionatto S. Antibacterial mechanisms of cinnamon and its constituents: A review. *Microb Pathog*. 2018;120:198-203. doi: 10.1016/j.micpath.2018.04.036